ASSESSMENT OF SEISMIC RISK FOR MUSEUM ARTIFACTS

C.C. Spyrakos [1], Ch.A. Maniatakis [2] and I.M. Taflampas [3]

[1] *Professor, Dept. of Civil Engineering, Laboratory for Earthquake Engineering National Technical University, Athens, Greece*

[2] *Civil Engineer, PhD Candidate, Dept. of Civil Engineering, Laboratory for Earthquake Engineering National Technical University, Athens, Greece*

[3] *Civil Engineer, Dept. of Civil Engineering, Laboratory for Earthquake Engineering National Technical University, Athens, Greece*

Email: spyrakos@hol.gr, chmaniat@mail.ntua.gr, taflan@central.ntua.gr

ABSTRACT:

The protection of several types of museum collections against seismic hazard is increasingly gaining the interest of scientists and governments, as their damage is in many cases irreparable. Special programs of earthquake preparedness are conducted in order to mitigate the expected hazard, especially for earthquake - prone countries, such as the countries of eastern Mediterranean. In this study several types of art object failures caused by earthquakes are presented and risk mitigation methods are described. The magnitudes of Peak Ground Acceleration (*PGA*) and Peak Ground Velocity (*PGV*) that can cause failure are determined for a sample of representative artifacts applying suitable criteria. Several earthquakes are considered to determine the distance from the causative fault at which failure is expected using appropriate attenuation relationships and theoretical models for both near- and far-fault regions.

KEYWORDS: museum artifacts, seismic risk, failure criteria, attenuation relationships, near-far fault regions

1. INTRODUCTION

1.1 Seismicity in Greece

The eastern Mediterranean Sea including Italy, Balkan countries, Cyprus and Turkey is well known for the noteworthy history of the native civilizations. These countries are not only celebrated for their cultural heritage, but also known for their high seismic activity.

There is an earthquake with a magnitude of at least 6 in the Richter scale every two years in Greece, the country with the highest seismicity in Europe. Fortunately, most of the earthquake epicenters are located offshore. However, there has been a number of strong earthquakes that have occurred near or at the mainland that have caused loss of life and severe damage to engineered structures. Representative strong earthquakes that have occurred in Greece during the last 80 years are listed in Table 1, in terms of the surface wave magnitude scale M_S.

Damages of both museum buildings and artifacts have been observed in many cases in Greece. The recent (1999) Athens earthquake not only caused severe damages to numerous engineered structures, but also to artifacts and statues in museums (figure 1.1). The 1999 Athens earthquake, with a magnitude defined as M_L=5.4 in the local magnitude scale and as M_S=5.9 in the surface wave magnitude scale, originated at a normal fault rupture with a focal depth of almost 12 km and at a distance of 18-20km from the historical centre of Athens. The event was unexpected since it occurred in a region traditionally considered as of low seismicity and there was no active fault mapped in the epicentral area. The earthquake mainly hit the northwestern Athens suburbs, which are close to the causative fault. More than 80 buildings collapsed, including industrial facilities, causing 143 deaths, while injuries were as many as 2000. About 60000 buildings suffered different levels of damage (slight to heavy). The tangible losses were roughly estimated at about 3 billions US dollars, and from this point of view it was the

worst natural disaster in modern Greek history. Significant failures of artifacts were observed also during the recent Kefalonia 2007 earthquake at the Argostoli museum (figure 1.2).

Table 1.1 Representative earthquake events in Greece

	Event	*Date*	M_S		*Event*	*Date*	M_S
1	Sparti	August 30, 1926	7.2	*7*	Kalamata	September 13, 1986	6.0
2	Ierissos	September 30, 1932	7.0	*8*	Aigion	June 15, 1995	6.4
3	Karpathos	February 9, 1948	7.1	*9*	Athens	September 7, 1999	5.9
4	Argostoli	August 12, 1953	7.2	*10*	Lefkas	August 14, 2003	6.4
5	Thessaloniki	June 20, 1978	6.5	*11*	Kithira	Jenuary 8, 2006	6.9
6	Alcyonides	February 24, 1981	6.7	*12*	Kefalonia	March 25, 2007	5.9

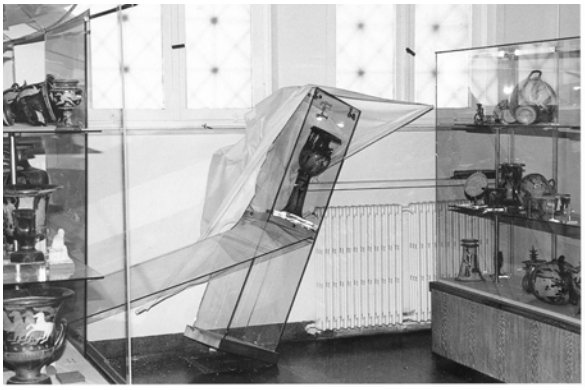

(1.1)

(1.2)

Figure 1 Failure examples of art objects and artifacts: (1.1) Failures caused by overturning at the National Museum of Athens during the 1999 Athens (Parnitha) earthquake (1.2) Failures caused by overturning and impact at the Archaeological Museum of Argostoli during the Kefalonia 2007 earthquake

The works of art were severely damaged by overturning or sliding and impact. The main reason for their failure was the fact that they were not anchored.

1.2 Mitigation Measures

One of the primary reasons for failures of building and artifacts is that no seismic code was enforced in Greece until 1959. However, seismic codes were enforced locally at certain regions in Greece at the beginning of the 19th century. The current Greek Seismic Code (EAK 2000) requires use of elastic spectra for artifacts with ordinates proportional to i) the maximum ground acceleration and ii) the importance factor that amplifies the design value by 30%. The code also recognizes the fact that the acceleration increases with height. It allows for either a dynamic analysis or an equivalent static analysis. For the latter the seismic load is applied as a static load at the center of gravity of the object, amplified by a factor which is proportional to the ground acceleration, depending on the height of the object from the foundation and the fundamental period of both the object and the structure.

In an effort to provide easily-applied directives, the Greek Ministry of Culture (2002) has published a series of guidelines concerning the design of support systems and display cases, as well as the application of the appropriate post-earthquake measures to the artifacts damaged by earthquakes.

A recent experimental investigation is presented in a report by Zampas *et al.* (2004) for the design of support systems in the Benaki Museum in Athens. Full-scale shake table tests were performed at the National Technical University of Athens (NTUA) Laboratory of Earthquake Engineering, in order to investigate the response of two replica artifacts and a replica vase, supported by a slender base. The artifacts were considered as representative for Greek museums. The tests revealed an amplification of the earthquake accelerations, as one moves from the base to the top of an object. Furthermore, the support pins exhibited permanent flexural deformations, which in turn resulted to tilting of the artifacts.

The use of isolators results in much lower accelerations applied to the art objects, and thus in a reduced damage potential. Despite the fact that base isolation is a method which can be considered cost-effective in cases of important statues or artifacts, its application in Greece is limited to a few cases, the most important being that of the Hermes statue at the Olympia museum (Koumousis, 2006).

Analytical studies of the dynamic response of six replica statues of the Archaeological Museum of Athens with the use of the Finite Element Method revealed weak areas and areas of high stress concentrations in regions with abrupt changes in geometry, such as connections of arms with statue body and statue ankles. Such regions that are susceptible to high stresses could be strengthened either by means of larger local thickness, or appropriate strengthening metal reinforcement.

2. ANALYSIS OF RIGID ARTIFACTS

In the present study the critical peak ground acceleration *PGA* and velocity *PGV* that can cause rocking and overturning, respectively, for the objects shown in Figure 2 are estimated. Sliding is not examined since it requires experimental measurement of the friction coefficient at the interface of the artifact and its supports. The analysis is based on the methodology introduced by Agbabian *et al.* (1990) for the evaluation of seismic mitigation measures in the J. Paul Getty Museum, as well as an analytical study of Spyrakos and Nikolettos (2005). Assuming that the earthquake response of an artifact can be adequately described using rigid body kinematics, three failure modes are identified: rocking, sliding and overturning.

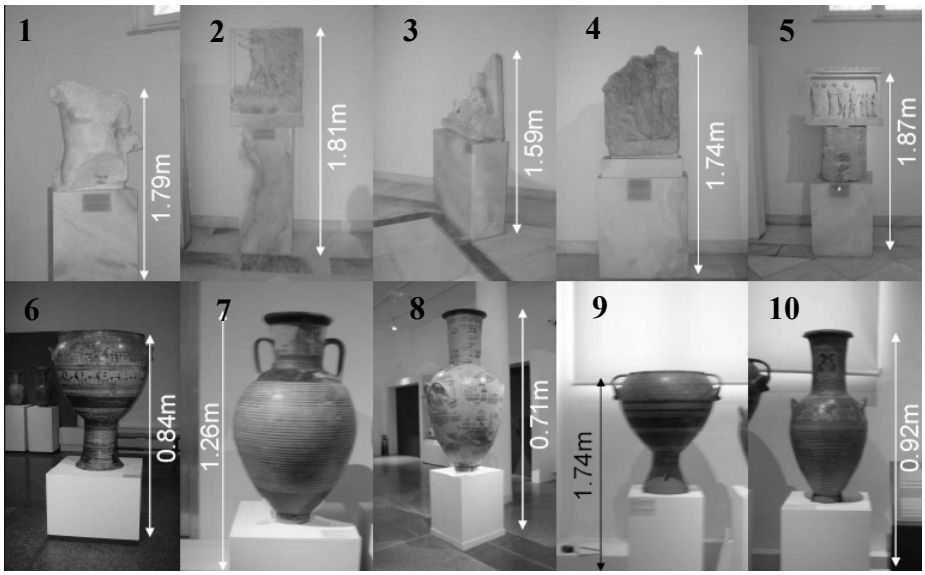

Figure 2 Artifacts placed at the ground (no. 1 to 5) and the first (no. 6 to 10) floor at the National Archaeological Museum of Athens for which a seismic hazard assessment has been carried out

The first two failure modes are controlled by the peak ground acceleration (*PGA*) and the peak ground velocity (*PGV*), respectively. According to Spyrakos and Nikolettos (2005), the overturning stability of a rigid structure is determined by the following criterion

$$\frac{B}{H} = \frac{S_{vo}}{\sqrt{gR}} \tag{2.1}$$

where S_{vo} is the spectral velocity required to cause overturning, B is the object width, H is the object height, g is the acceleration of gravity and R=0.5(B^2+H^2)$^{1/2}$.

The criteria for the three modes of failure (Agbabian *et al.* 1990) are:

$$\frac{A}{g} \geq \frac{B}{H'} \text{(Rocking)}, \quad V \geq 10\frac{B}{\sqrt{H'}} \text{(Overturning)}, \quad \frac{A}{g} \geq C \text{(Sliding)} \tag{2.2}$$

where A and V are the maximum horizontal acceleration and velocity at the base of the object, respectively, B is the object base width, C the friction coefficient and H' an "equivalent object height" defined for complex object geometries. This "equivalent height" depends on the art object area, second moment of inertia about a horizontal axis at the ground level and vertical distance of center of gravity from the ground level. Equations 2.2 define the thresholds of horizontal acceleration (A) and velocity (V) that can cause failure. The *PGA* and *PGV* values required for rocking or overturning are listed in Table 2.

Table 2.1 Critical values of *PGA* and *PGV* for rocking and overturning, respectively

Artifact No	*PGA (g)*	*PGV (cm/sec.)*	*Artifact No*	*PGA (g)*	*PGV (cm/sec.)*
1	0.189	36.11	*6*	0.117	13.12
2	0.139	27.18	*7*	0.231	31.56
3	0.286	51.33	*8*	0.265	27.04
4	0.168	30.53	*9*	0.128	18.79
5	0.122	23.17	*10*	0.135	14.96

3. HAZARD ESTIMATION

A procedure to estimate the seismic risk involves the correlation of the *PGA* and *PGV* with the epicentral distance and the earthquake magnitude, in conjunction with the knowledge of active faults and historical seismicity in the area of interest. Such a procedure allows for a preliminary assessment of the need to resort to further mitigation measures.

In the present study, the empirical attenuation relations by Theodulidis and Papazachos (1992) were employed. These expressions relate *PGA* and *PGV* with the epicentral distance R and surface wave magnitude M_S, according to the following equations:

$$\ln(PGA) = 3.88 + 1.12M_S - 1.65 \cdot \ln(R+15) + 0.41 \cdot S \tag{3.1}$$

$$\ln(PGV) = -0.79 + 1.41M_S - 1.62 \cdot \ln(R+10) - 0.22 \cdot S \tag{3.2}$$

where R the epicentral distance in km and S a Boolean parameter that is equal to one for rock sites and zero for alluvium sites. The *PGA* and *PGV* are expressed in cm/sec^2 and cm/sec, and related graphs are shown in figure 3.

In order to demonstrate the application of the methodology, the epicentral distances were estimated for three different earthquake magnitudes: M_S = 5.5, M_S = 6.5 and M_S = 7.5, and for two soil conditions, that is rock and

alluvium deposits, as shown in figure 3.

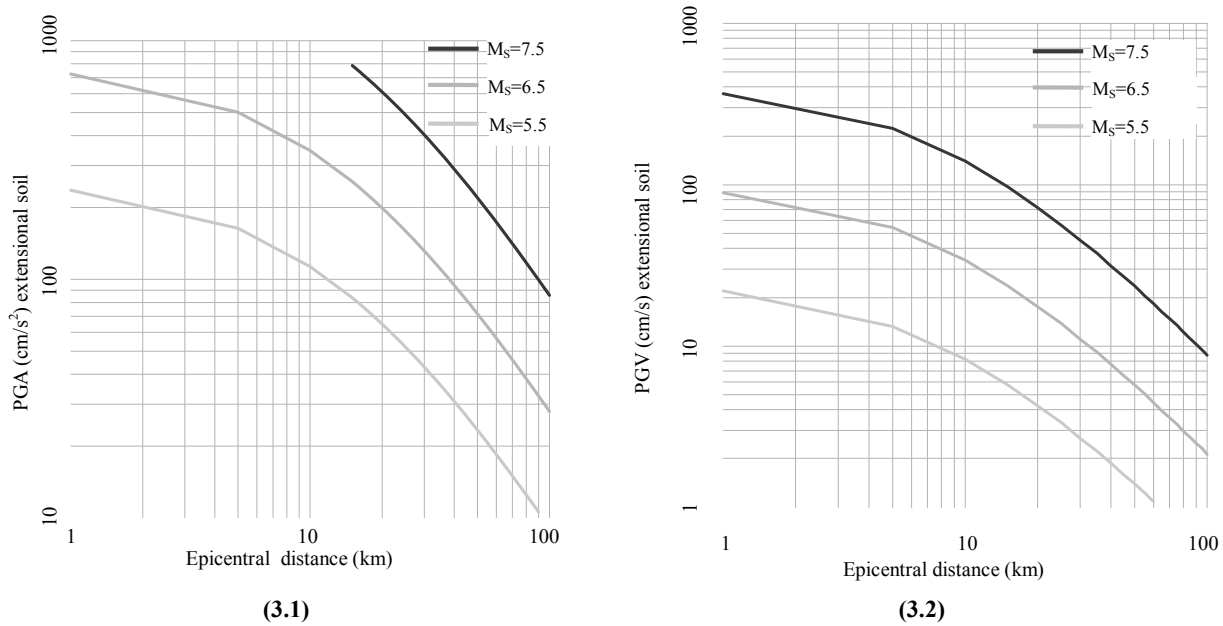

(3.1) **(3.2)**

Figure 3 Evaluation of the critical *PGA* (3.1) and *PGV* (3.2) values according to the relationships of Theodulidis and Papazachos (1992) for soft soil conditions

The work of Theodulidis and Papazachos (1992) is based on both near- and far-fault earthquake records. In order to account for near-source effects, the epicentral distances required for overturning failure, which involves the estimation of *PGV*, were also determined using three other empirical relationships proposed in the literature:

i) The relationship developed by Somerville (1998) in the near-fault zone is based on a sample of 15 recorded time histories and 12 simulated time histories. The records correspond to a magnitude range M_W = 6.2-7.5 and a distance from the fault rupture in the range of r=3-10 km. A distance cutoff of 3 km has been considered to avoid unrealistic predictions of *PGV* at short distances. The *PGV* is calculated as follows:

$$\ln(PGV) = -2.31 + 1.15M_W - 0.50 \cdot \ln(r) \tag{3.3}$$

ii) A similar relationship proposed by Alavi and Krawinkler (2000) is based on the same sample as the work of Somerville (1998). The *PGV* is calculated as follows:

$$\ln(PGV) = -5.11 + 1.59M_W - 0.58 \cdot \ln(r) \tag{3.4}$$

iii) The relationship developed by Rodriguez-Marek (2000) is based on 48 velocity time histories from 11 events. The data include earthquake records with distance r closest to the fault and less than 20 km, and a magnitude of M_S = 6.1-7.4. The *PGV* is calculated as follows:

$$\ln(PGV) = 2.44 + 0.50M_S - 0.41 \cdot \ln(r^2 + 3.93^2) \tag{3.5}$$

Also for the evaluation of *PGA* and *PGV* in the near- and far-fault region, a stochastic approach has been used with the aid of the Specific Barrier Model, proposed by Papageorgiou and Aki (1983a and b). Halldorsson and Papageorgiou (2005) incorporated a calibration of the Specific Barrier Model reflecting the characteristics of different tectonic regimes in the SGMS code. This code has been used to estimate the attenuation relationships for extentional regimes, such as the Hellenic (Aegean) arc, and Turkey, and extensional regimes, such as the

continental Greece. Stiff rock conditions (shear wave velocity V_{30} = 940 m/s for extensional regimes and V_{30} = 620 m/s for inter-plate regimes) and site classifications D and C have been considered according to NEHRP Provisions (BSSC, 1998). The estimation of the Joyner-Boore distance for "critical" PGA and PGV values that is capable to provoke rocking or overturning, respectively, for inter-plate regimes is shown in figure 4.

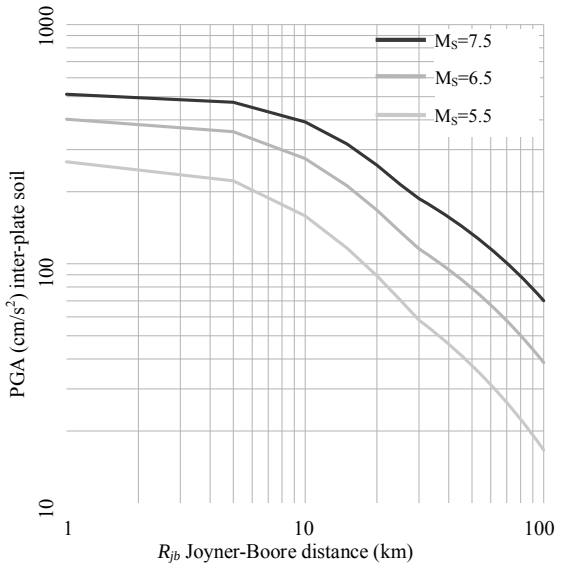

(4.1)

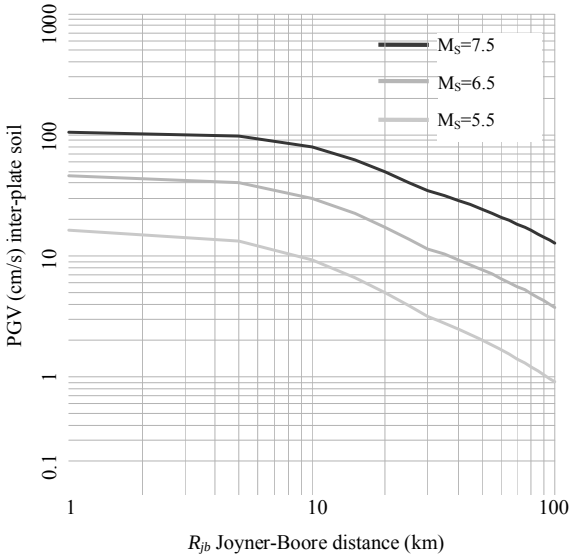

(4.2)

Figure 4 Evaluation of the critical *PGA* (4.1) and *PGV* (4.2) values for inter – plate regimes based on the Specific Barrier Model and soft soil conditions

Utilizing Eqns. 3.1, 3.2, 3.3, 3.4 and 3.5, the radii from the epicenter defining areas of expected rocking or overturning failures, are calculated. Indicative results for the artifacts of the ground and the first floor are presented in Tables 3.1 and 3.2, respectively, considering M_S, M_W=6.5.

Table 3.1 Critical values of distance in km for M_S, M_W=6.5 for the artifacts of the ground floor

	Theodulidis & Papazachos (M_S-R_{ep})		***Halldorsson & Papageorgiou (inter-plate) (M_S-R_{jb})***		***Halldorsson & Papageorgiou (extensional) (M_S-R_{jb})***	
Artifact No.	*rock*	*soil*	*rock*	*soil*	*rock*	*soil*
1	32.0	21.5	16.0	18.0	5.5	12.0
2	41.5	29.0	22.0	25.0	10.5	18.0
3	21.5	13.5	9.0	10.0	●	3.0
4	35.0	24.0	18.5	20.5	7.5	14.0
5	46.0	32.5	25.0	29.0	13.0	20.5

Artifact No.	***Somerville (M_W-R_{fr})***	***Alavi & Krawinkler (M_W-R_{fr})***	***Rodriguez & Marek (M_S-R_{cf})***
1	23.5	17.0	12.0
2	×	27.5	18.0
3	11.5	9.0	7.5
4	33.0	22.5	15.5
5	×	×	22.0

×: distance R greater than 20km (object overturned in the near-fault area)
●: failure not reached
R_{ep}**:** epicentral distance; R_{jb}**:** Joyner-Boore distance; R_{fr}**:** distance from the fault rupture; R_{cf}**:** distance closest to the fault

The critical distances at which failure occurs, as estimated by Eqns. 3.1 and 3.2, appear to be significantly greater than the distances obtained from the other relationships. This difference is attributed to the characteristics of the sample of earthquake records and probably to the lack of sufficient number of strong motion data at small distances from the fault. The distances resulting from the Specific Barrier model are in close agreement with the results of Eqns. 3.5, 3.6 and 3.7; however, significant distortion of the results is observed. The artifacts of the first floor are threatened with failure from epicenters located in greater distances compared with the objects placed in the ground floor, as expected. The cases of failure at distances smaller than 20 km indicate the vulnerability of artifacts in the near-fault region, even without considering the special characteristics of the strong motion in that area of interest (Sommerville, 1998, Spyrakos *et al.*, 2008). The strong motion characteristics of the zone characterized as "near-source" are strongly influenced by the fault rupture mechanism and the rupture propagation direction with respect to the site's location, as well as permanent displacement phenomena attributed to the fault slip. When the fault rupture propagates towards the site of interest, a seismic energy concentration occurs, resulting in the occurrence of a velocity pulse in the direction normal to the fault plane (Sommerville *et al.*, 1997). Significant failures have been addressed even for the case of M_S, M_W=5.5.

Table 3.2 Critical values of distance in km for M_S, M_W=6.5 for the artifacts of the first floor

	Theodulidis & Papazachos (M_S-R_{ep})		***Halldorsson & Papageorgiou (inter-plate) (M_S-R_{jb})***		***Halldorsson & Papageorgiou (extensional) (M_S-R_{jb})***	
Artifact No.	*rock*	*soil*	*rock*	*soil*	*rock*	*soil*
6	48.0	34.0	26.0	30.5	13.5	22.0
7	26.5	17.5	13.0	14.0	●	8.0
8	23.0	15.0	10.5	12.0	●	8.5
9	44.5	31.0	24.0	27.5	12.0	19.5
10	42.5	30.0	22.5	26.0	11.0	19.0
Artifact No.	***Somerville (M_W-R_{fr})***		***Alavi & Krawinkler (M_W-R_{fr})***		***Rodriguez & Marek (M_S-R_{cf})***	
6	×		×		×	
7	31.0		21.0		15.0	
8	×		28.0		18.0	
9	×		×		28.5	
10	×		×		×	

×: distance R greater than 20km (object overturned in the near-fault area)
●: failure not reached
***R_{ep}*:** epicentral distance; ***R_{jb}*:** Joyner-Boore distance; ***R_{fr}*:** distance from the fault rupture; ***R_{cf}*:** distance closest to the fault

4. CONCLUSIONS

Seismic mitigation for art objects has rather been poorly addressed in most countries. Specific measures have been taken in Greece, especially after the recent 1999 earthquake. New promising technologies, such as base isolation, have been recently applied to certain special occasions. However, the experimental investigation of art objects behavior and the performance of seismic risk analysis of museums has been limited.

The significant vulnerability of artifacts in the near-fault region, even for small to moderated earthquake magnitudes is addressed. More vulnerable areas are the regions near inter-plate regimes, such as the Hellenic arch and Turkey. Critical distances are overestimated using attenuation relations based on time-history samples from far-field regions. The Specific Barrier model approximation results in more "rational" values of *PGA* and *PGV* in the near-fault region. Significant differences in the attenuation relations are observed.

Further analytical studies and experimental work is needed to assess the hazard of artifacts considering near-fault effects.

ACKNOWLEDGEMENTS

The research of Ch.A. Maniatakis is funded by a doctoral scholarship from *Alexander S. Onassis* Public Benefit Foundation. This financial support is gratefully acknowledged.

REFERENCES

Agbabian, M.S., Masri, S.F. and Nigbor, R.L. (1990). Evaluation of Seismic Mitigation Measures for Art Objects, The J.P. Getty Trust, USA.

Earthquake Planning and Protection Organization (OASP) (2000). Greek Seismic Code EAK 2000 (In Greek), Athens, Greece.

Building Seismic Safety Council (BSSC), (1998), 1997 NEHRP Recommended Provisions for the Development of Seismic Regulation for New Buildings, Federal Emergency Management Agency, Washington, DC, FEMA 302.

Ghiossi, S., Krini, M., Maragou T. and Prokos, P. (2002). Earthquakes and Ancient Artifacts - Prevention and Post-Earthquake Mitigation Measures (In Greek), Greek Ministry of Culture, Athens.

Halldorsson, B. and Papageorgiou, A.S. (2005). Calibration of the specific barrier model to earthquakes of different tectonic regions. *Bulletin of the Seismological Society of America* **95**, 1276–1301.

Koumousis, V. (2006). Seismic Isolation System for the Statue of Hermes at the New Museum of Olympia, J. Paul Getty Museum, 3-4 May 2006, Los Angeles, USA.

Papageorgiou, A.S. and Aki, K., (1983a). A Specific Barrier model for the quantitative description of inhomogeneous faulting and the prediction of strong ground motion. I. Description of the model. *Bulletin of the Seismological Society of America* **73**, 693–722.

Papageorgiou, A.S. and Aki, K., (1983b). A Specific Barrier model for the quantitative description of inhomogeneous faulting and the prediction of strong ground motion. Part II. Applications of the model. *Bulletin of the Seismological Society of America* **73**, 953–978.

Rodriguez-Marek, A. (2000). Near-Fault Seismic Site Response. Ph.D. Dissertation, Civil Engineering Department, University of California at Berkeley.

Somerville, P.G., Smith, N.F., Graves, R.W. and Abrahamson, N.A. (1997). Modification of Empirical Strong Ground Motion Attenuation Relations to Include the Amplitude and Duration Effects of Rupture Directivity. *Seismological Research Letters* **68:1**, 199-222.

Spyrakos, C.C. and Nikolettos, G.S. (2005). Overturning stability criteria for flexible structures to earthquakes. *ASCE Journal of Engineering Mechanics* **131:4**, 349-358.

Spyrakos, C.C., Maniatakis, Ch. A. and Taflambas, J. (2008). Evaluation of near source seismic records based on damage potential parameters. Case study: Greece. *Soil Dynamics & Earthquake Engineering* **28**, 738-753.

Theodulidis, N.P. and Papazachos, B.C. (1992). Dependence of strong ground motion on magnitude-distance, site geology and macroseismic intensity for shallow earthquakes in Greece: I, Peak ground acceleration, velocity and displacement. *Soil Dynamics and Earthquake Engineering* **11**, 387-402.

Zampas, K., Chatziantoniou, K., Galanou, A. and Dogani, A. (2004). Protection of Ancient Artifacts Against Earthquakes (In Greek), Research Project Final Report, Organization for Aseismic Design and Protection, Athens, Greece.